

Preparation and characteristics of Bi–Pb–Sr–Ca–Cu–O superconducting films by spray pyrolysis and post-annealing

Hong-Show Koo, Tseung-Yuen Tseng *

Department of Electronics Engineering and Institute of Electronics, National Chiao-Tung University, Hsinchu, Taiwan

Received 10 November 1997; received in revised form 20 June 1998; accepted 22 June 1998

Abstract

Two kinds of high- T_c superconducting films, $\text{Bi}_{1.8}\text{Pb}_{0.2}\text{Sr}_2\text{Ca}_2\text{Cu}_3\text{O}_y$ and $\text{Bi}_2\text{PbSr}_2\text{Ca}_2\text{Cu}_3\text{O}_y$, were prepared by spray pyrolysis and post-annealing with the aid of Bi-based bulk. Highly c -oriented and nearly single-phase 2223 high- T_c Bi-based superconducting films can be achieved for the as-sprayed $\text{Bi}_{1.8}\text{Pb}_{0.2}\text{Sr}_2\text{Ca}_2\text{Cu}_3\text{O}_y$ and the $\text{Bi}_2\text{PbSr}_2\text{Ca}_2\text{Cu}_3\text{O}_y$ films annealed at 845°C for 20 h. X-ray diffraction (XRD) patterns exhibit amorphous-like phases with microcrystals for the as-sprayed films and the transformation of amorphous-like phase into crystalline high- T_c (2223), low- T_c (2212) and Ca_2PbO_4 phases for the resultant films. For as-sprayed films, post-annealing in the closed system with Bi-based bulk sources is favourable to the formation of 2223 phase; on the contrary, the 2212 phase is formed in the open system, as demonstrated by XRD and scanning electron microscopy (SEM). SEM and XRD analyses show a plate-like microstructure for the 2223 phase and a needle-like one for the 2212 phase. This phenomenon explains that compensation and diffusion of Bi-based bulk sources into the as-sprayed films help in the formation of 2223 phase and these processes are more efficient in the closed system. The resultant film shows a high critical transition temperature ($T_{c,zero}$) of 104 K and a critical current density (J_c) of 1.8×10^4 A/cm². © 1998 Elsevier Science S.A. All rights reserved.

Keywords: Spray pyrolysis; Bi-based superconductors; Superconducting films; Amorphous; Transformation; Plate-like microstructure; Needle-like microstructure

1. Introduction

High- T_c oxide superconducting thin film is one of the most promising candidates for fabricating active/passive devices and has excellent potential for microelectronic and microwave applications. Superconducting thin-film preparation technology plays a key and indispensable role in the fabrication of electronic devices. To date, various processing methods for high- T_c superconducting Y–Ba–Cu–O, Bi(Pb)–Sr–Ca–Cu–O and Tl–Ba–Ca–Cu–O films have been extensively attempted and films have been successfully prepared by physical and chemical deposition techniques such as sputtering [1], molecular beam epitaxy [2], evaporation [3], chemical vapour deposition [4] and laser ablation [5].

Expensive, sophisticated and specialized apparatus is needed to prepare the desired superconducting films via the above-mentioned processes. From the viewpoint of economy and efficiency, other kinds of chemical processes such as sol-gel and spray pyrolysis have also been paid particular atten-

tion for preparing films with various shapes. The sol-gel technique have been extensively used to synthesize superconducting oxide powders, fibres and films, but some previous work shows that the spray pyrolysis technique is mostly limited to the preparation of Y–Ba–Cu–O film and powder [6,7] and ceramic powders including superconductors [8].

For the Bi–Sr–Ca–Cu–O system, the coexistence of three phases, $\text{Bi}_2\text{Ca}_2\text{CuO}_y$ (2201), $\text{Bi}_2\text{Sr}_2\text{CaCu}_2\text{O}_y$ (2212) and $\text{Bi}_2\text{Sr}_2\text{Ca}_2\text{Cu}_3\text{O}_y$ (2223), with T_c s of 20, 80 and 110 K, respectively, has often been found in the preparation of thin films and bulks. Various attempts, such as addition of Ca_2PbO_4 catalyst [9] and excess CuO/CaO [10], low-temperature annealing and a deposition atmosphere of O_2/Ar [11] with different ratios, have been tried to prepare high- T_c superconducting thin films and bulks with nearly single-phase $\text{Bi}_2\text{Sr}_2\text{Ca}_2\text{Cu}_3\text{O}_y$ of $T_c = 110$ K. Yamada and Murase [12] reported that the addition of Pb to the Bi–Sr–Ca–Cu–O compound enhanced the formation of a single phase with $T_c \sim 110$ K. Endo et al. [11] demonstrated that the reaction under low oxygen pressure has the effect of lowering the heat-treatment temperature with broad ranges to render the high- T_c phase of Bi–Sr–Ca–Cu–O with a superconducting transition at 107.5

* Corresponding author. Fax: 886-3-5724361; E-mail: tseng@cc.nctu.edu.tw

K. The spray-pyrolysis [13] technique is a simple, convenient, versatile and low-cost process for the preparation of thin-film oxides such as Y–Ba–Cu–O [6,14], Bi–Sr–Ca–Cu–O [15] and Tl–Ba–Ca–Cu–O [16]. There are very few reports on the preparation of single-phase (2223) Bi(Pb)–Sr–Ca–Cu–O thin film with $T_c \sim 110$ K [17,18]. Manabe et al. [19] prepared superconducting films with 2223 phase by the dipping-pyrolysis technique with metal naphthenates in toluene, and the resultant film showed a $T_{c,zero} \sim 106$ K and $J_c(77$ K) $\sim 2 \times 10^3$ A/cm². High- T_c superconducting films of 2212 and 2223 phases with a $T_{c,zero}$ of 104 K and $J_c(77$ K) of 7.5×10^6 A/m² prepared by spinning-coating/dipping pyrolysis with metal carboxylates [20] were also reported in the literature.

In this work, we have applied a spray-pyrolysis method using metal nitrates as starting materials and glycerol as solvent to prepare the as-sprayed film. The films were post-annealed with Bi(Pb)-based bulk sources. The influence of optimal processing parameters on the formation of the superconducting single-phase (2223) oxide thin film in the Bi-based system with $T_c \sim 110$ K was investigated. The role of compositional and microstructural variation of the films on the physical characteristics was also studied in detail.

2. Experimental

Films with two different compositions, Bi_{1.8}Pb_{0.2}Sr₂Ca₂Cu₃O_y (film A) and Bi₂PbSr₂Ca₂Cu₃O_y (film B), were prepared from a glycerol solution consisting of the high-purity compounds Bi(NO₃)₃·5H₂O, Pb(NO₃)₂, Sr(NO₃)₂, Ca(NO₃)₂·4H₂O and Cu(NO₃)₂·3H₂O. The as-sprayed films were formed on MgO substrates heated at 150–200°C by spraying the solution using a spray gun. The distance between the nozzle orifice and the substrates was about 15 cm and the typical thickness of the as-sprayed films was about 20–30 μm. The as-sprayed films were annealed for 5 h at 300, 500, 700 and 800°C. The as-sprayed films were also annealed at temperatures between 840 and 850°C for 5, 10, 20, 25 and 50 h to find out the optimal conditions for the preparation of films with high T_c . All as-sprayed films were processed in a closed system with Bi_{0.8}Pb_{0.2}SrCaCu₂O_y bulk sources. Superconducting Bi_{0.8}Pb_{0.2}SrCaCu₂O_y bulks were prepared by the solid-state reaction process. For comparison of critical transition temperature and volume fraction of 2223 phase in the films, the as-sprayed films A were annealed at 845°C for various periods in closed and open systems. The closed system means that the as-sprayed film and bulk source were put together inside a crucible with a cover, whereas the open system uses an uncovered crucible. Thermal characteristics of the as-sprayed powders, which were scratched from the as-sprayed films on the substrates, were analysed using differential thermal analysis (DTA) and thermogravimetry (Sinku-Riko/TGD 7000). The phases in the as-sprayed and resultant films were identified using a Philips PW 1700 X-ray diffractometer with nickel-filtered Cu K α radiation (40

kV, 30 mA) at a scan rate of 0.04°/s with scan angles (2θ) ranging from 3 to 60°.

The thickness, surface morphology and composition of the as-sprayed and resultant films were examined under a Cam-scan scanning electron microscope equipped with an energy-dispersive X-ray analyser (EDXA) and inductively coupled plasma-atomic emission spectrometer (ICP-AES). For the electrical resistance measurement, a standard four-point probe technique was employed. The measured data were acquired and analysed using an IBM PC-AT computer. Electrical contacts to the films were made using fine copper leads attached to the films with a conductive silver paste. The resistance limit measured was 10^{-6} Ω. The critical current densities of the resultant films were measured with a nanovoltmeter model 181 and a voltage/d.c. current power-supply source model 228 from Keithley. Similarly, a four-point technique was also employed to measure the transport critical current density with a criterion of 1 μV/cm.

3. Results and discussion

3.1. The Bi_{1.8}Pb_{0.2}Sr₂Ca₂Cu₃O_y film (film A)

The solid curves in Fig. 1 show the thermal characteristics of the Bi_{1.8}Pb_{0.2}Sr₂Ca₂Cu₃O_y powders which were scratched from the as-sprayed films. A large broad exothermic peak at 100–300°C shows a minor weight loss due to the evaporation of mist and partial decomposition of nitrates into carbonates, whereas the other small broad exothermic peak and the 3.2% weight loss appearing at a temperature of 600–700°C correspond to the complete decomposition of residue nitrates. Three exothermic peaks appeared at the temperatures around 800, 835 and 850°C, respectively, with various reaction heats and the weight loss finally approached a constant value of 9.39%. These exothermic peaks indicated that the reaction, formation and melting phenomena of high- T_c superconduct-

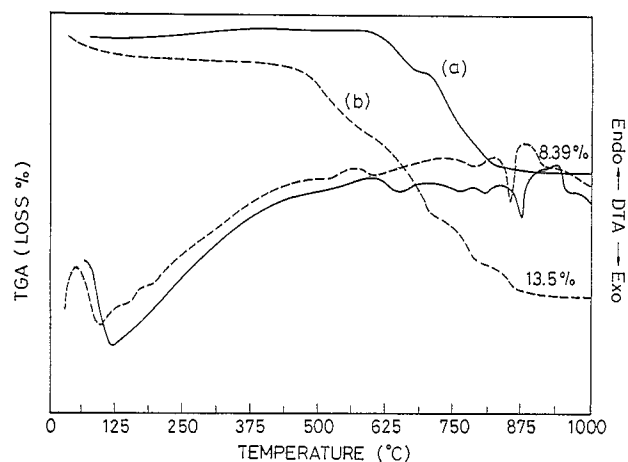


Fig. 1. Thermal characteristics of (a) Bi_{1.8}Pb_{0.2}Sr₂Ca₂Cu₃O_y (solid line) and (b) Bi₂PbSr₂Ca₂Cu₃O_y (dashed line) powders scratched from the as-sprayed films.

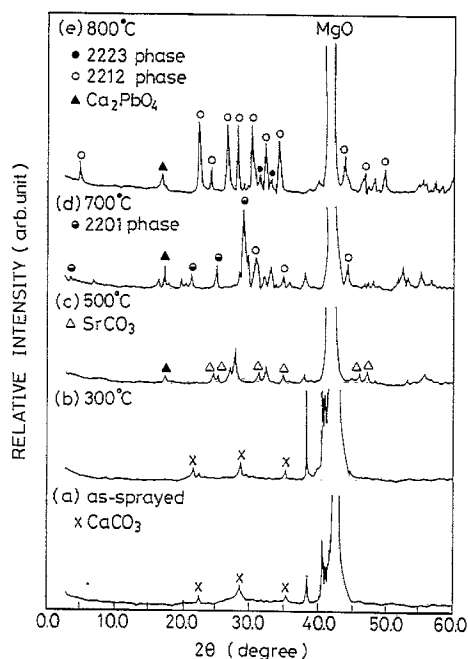


Fig. 2. XRD patterns of the films A: as-sprayed (a) and annealed at 300°C (b), 500°C (c), 700°C (d) and 800°C (e) for 5 h.

ing oxides probably occur at about 800, 835 and 850°C; this is supported by the XRD results.

Fig. 2 shows XRD patterns of the as-sprayed film (a) and films A annealed at 300°C (b), 500°C (c), 700°C (d) and 800°C (e) for 5 h. The CaCO₃ phase merely appears for the

as-sprayed film A and in the film A annealed at 300°C, which is consistent with the exothermic reaction observed at 100–300°C in the thermal characteristics and proved that the nitrates can be easily decomposed and the carbonates formed at lower temperatures. The film A annealed at 500°C shows the appearance of SrCO₃ and Ca₂PbO₄ phases. Furthermore, in the films A annealed at 700 and 800°C, the existence of phases of Ca₂PbO₄, Bi₂Sr₂CuO_y (2201) with a T_c of 20 K, 2212 with a T_c of 80 K and 2223 with a T_c of 110 K were identified. The relative intensity of the Ca₂PbO₄ phase gradually increased as the annealing temperature was increased from 500 to 800°C, which indicated that the formation of the intermediate phase of Ca₂PbO₄ occurred at below 800°C, but it will be decreased as the annealing temperature increases above 800°C, as shown in Fig. 9. The phase of Bi₂Sr₂CuO_y (2201) with minor peaks of Ca₂PbO₄ and 2212 was formed as the major phase at 700°C (Fig. 2). On the other hand, the formation of major low- T_c 2212 and minor high- T_c 2223 phases was observed in the film A annealed at 800°C. These results show that major 2223 phase is difficult to form below 800°C, but it appears at temperatures higher than 800°C or for longer annealing times. SEM photographs of the as-sprayed film (a) and films A annealed at 500°C (b), 700°C (c) and 800°C (d) for 5 h are shown in Fig. 3. A flock-like morphology is observed for the as-sprayed films. More pores seen in the films annealed at 500°C (b) and 700°C (c) indicate that the evaporation and decomposition of nitrates and carbonates occurred during the reaction. The morphology of

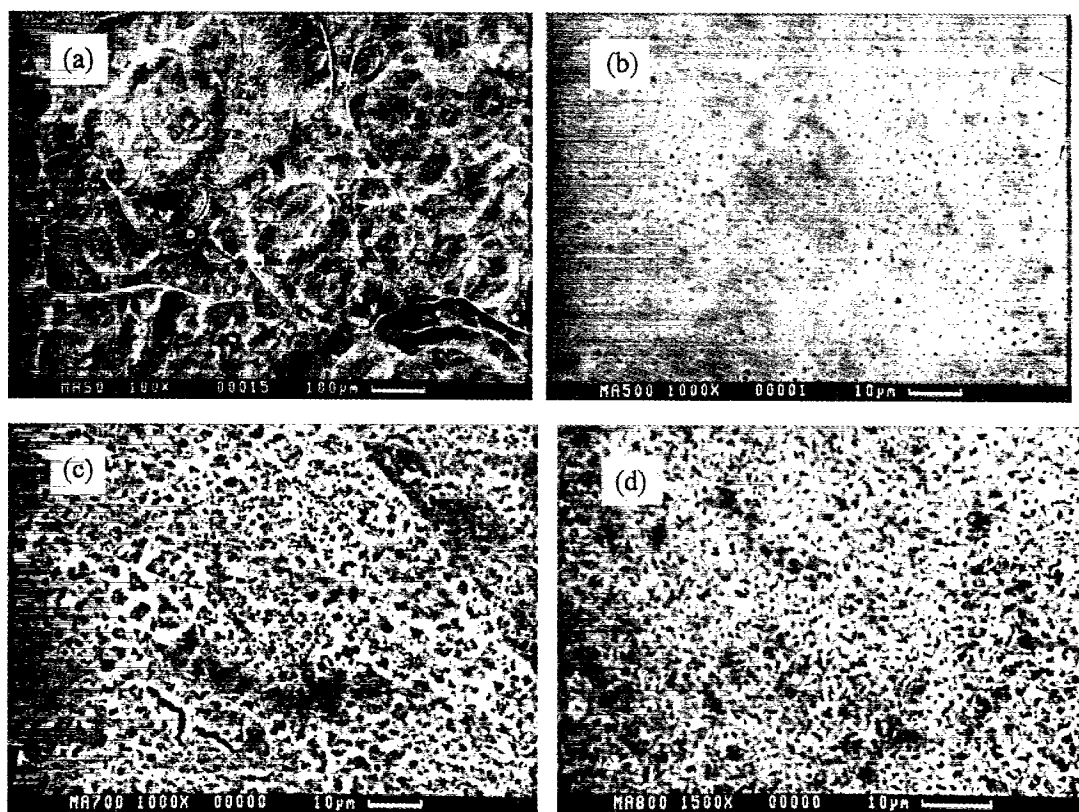


Fig. 3. SEM photographs of the films A: as-sprayed (a) and annealed at 500°C (b), 700°C (c) and 800°C (d) for 5 h.

the resultant films annealed at 800°C shows a needle-like microstructure with the characteristics of a low- T_c 2212 phase (Fig. 3(d)), as demonstrated by Fig. 2(e).

XRD patterns of the films A annealed at 845°C for 5 h (a), 10 h (b), 20 h (c) and 50 h (d) are shown in Fig. 4. Fig. 4(a) and (b) indicates the coexistence of 2223 and 2212 phases, and the formation of highly oriented single-phase 2223 occurred in the films A annealed at 845°C for 20 and 50 h (Fig. 4(c) and (d)). Similarly, a highly oriented single 2223 phase was also formed in the film B annealed at 845°C for 20 h, but annealing at 845°C for 5, 10 and 50 h showed the presence of multiple phases of 2223 and 2212.

Fig. 5(a) and (b) shows, respectively, the critical transition temperatures ($T_{c,zero}$) and volume fraction of the high- T_c 2223 phase of the as-sprayed films A annealed at 840, 845 (in closed and open systems) and 850°C, for various durations. The high critical transition temperature of 100 K was achieved for the films A annealed at 840°C/10–25 h and 845°C/25 h in the closed system and the volume fraction of high- T_c 2223 phase also increases with increasing treatment time. Further increase of the annealing temperature resulted in the formation of a low- T_c 2212 phase and hence a decrease in the critical transition temperature ($T_{c,zero}$) of the films. The comparison of the films annealed at 845°C in the closed and open systems shows the variation of the relative amount of superconducting phases and critical transition temperatures in the resultant films. The as-sprayed film with $\text{Bi}_{0.8}\text{Pb}_{0.2}\text{SrCaCu}_2\text{O}_y$ bulk in the closed system is favourable for the formation of the high- T_c 2223 phase. When the as-sprayed film was annealed in the open system, as indicated in Fig. 5, the low- T_c 2212 phase in the resultant films increased with increasing processing time and resulted in low critical transition temperatures of 17–24 K. The difference in the characteristics of the resultant films is ascribed to the compensation effect of Bi and Pb from the $\text{Bi}_{0.8}\text{Pb}_{0.2}\text{SrCaCu}_2\text{O}_y$ bulk source on the as-sprayed films and the prevention of evaporation of bismuth and lead during post-annealing in the closed system. The addition of appropriate amounts of lead has proved to be one of the effective techniques to promote the formation of the high- T_c 2223 phase [9].

Fig. 6 indicates the SEM morphologies of the films A annealed at 840 and 850°C for 5 and 50 h. The films annealed for a short duration both show needle-like and plate-like microstructures (Fig. 6(a) and (c)), while the size of the plate-like microstructure gradually increased and needle-like microstructure gradually decreased with increasing processing time (Fig. 6(b) and (d)). Two distinct surface microstructures of the films A annealed at 845°C for 5 and 50 h in closed and open systems are shown in Fig. 7. All plate-like morphologies existed in the films annealed in the closed system (Fig. 7(a) and (b)), while needle-like ones appeared in the films annealed in the open system (Fig. 7(c) and (d)). Kanai et al. [21] have proved that needle-like and plate-like surface microstructures should be characteristic of low- T_c 2212 and high- T_c 2223 phases, respectively.

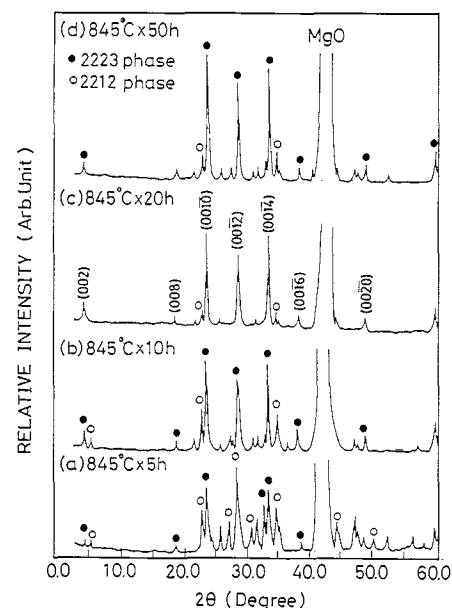


Fig. 4. XRD patterns of the films A annealed at 845°C for 5 h (a), 10 h (b), 20 h (c) and 50 h (d). The highly oriented and single-phase 2223 films were formed by annealing at 845°C for 20 h and 50 h.

Fig. 8 shows typical electrical resistance versus temperature relationships of the films A annealed at 840°C for 5 h (a), 10 h (b), 20 h (c), 25 h (d) and 50 h (e). The electrical resistance initially decreases with decreasing temperature and rapidly drops for a further decrease in the temperature, achieving zero resistance at the critical transition temperature. The zero-resistance critical transition temperature increases with increasing processing time up to a saturation value of around 100 K. Similar resistance-temperature relationships appear in the films A annealed at 845 and 850°C for various periods in the closed system. One-step and two-step transitions in the relationships of electrical resistance and temperature revealed the coexistence of high- T_c 2223 and low- T_c 2212 phases in the resultant films.

3.2. The $\text{Bi}_2\text{PbSr}_2\text{Ca}_2\text{Cu}_3\text{O}_y$ film (film B)

The dashed curves in Fig. 1 depict the thermal characteristics of the $\text{Bi}_2\text{PbSr}_2\text{Ca}_2\text{Cu}_3\text{O}_y$ powders which were scratched from the as-sprayed films. The broad exothermic peak at 100–200°C shows a minor weight loss of 1.25%, which corresponds to the evaporation of mist and partial decomposition of nitrates into carbonates; the other small exothermic peaks correspond to 10.0% weight loss with a stepped variation appearing around 500–750°C, which shows the complete decomposition of residual nitrates. Following these, two exothermic peaks appear at the neighbouring temperatures of 803 and 850°C with various reaction heats and gradual weight loss that may be due to the decomposition of the residual carbonates formed during the pyrolysis reaction; finally, a constant weight loss of ~13.5% is approached. The reaction, formation and partial melting phenomena of superconducting oxides may occur at about 850°C. The thermal

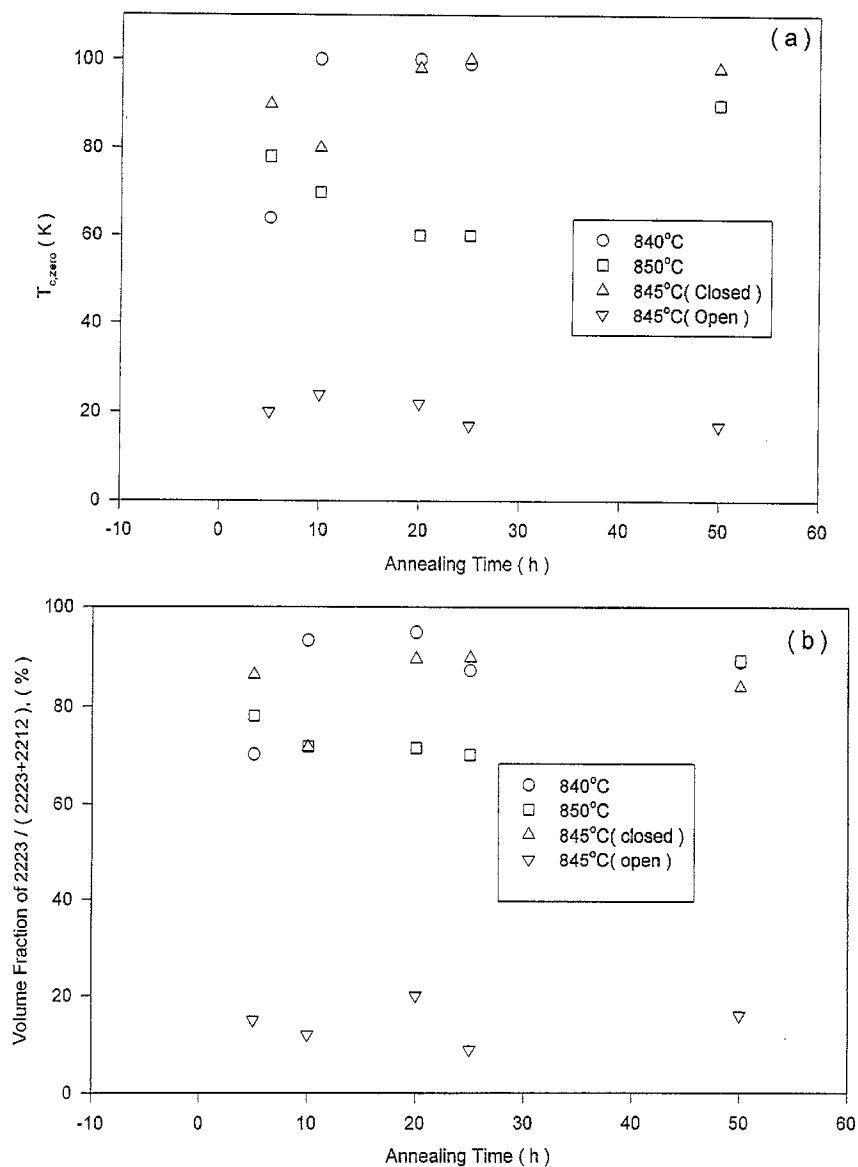


Fig. 5. (a) The critical transition temperature ($T_{c,zero}$) and (b) the volume fraction of high- T_c 2223 phase of the films A annealed at 840, 845 (in closed and open systems) and 850°C, for 5, 10, 20, 25 and 50 h.

characteristics of films A and B are similar, although the exothermic peaks appear at different temperatures and the extent of reaction heat is different. This is attributed to the difference in the stoichiometric ratio of (Bi + Pb) / Sr, namely 1.0 for film A and 1.5 for film B, hence resulting in the change in thermal reaction and appearance of the peaks. Since the formation reaction and annealing temperatures of the superconducting film are near its melting temperature, the composition is likely to change because of component vaporization, especially in a thin film during fabrication. The vaporization of Ba and Cu constituents in YBaCuO and of Bi, Pb and Cu components in BiSrCaCuO and BiPbSrCaCuO systems in atmospheres of O_2 , air and N_2 has been reported in the literature [22,23] and vapour pressures for Cu are higher and those for both Bi and Pb are lower than the values estimated from as-sprayed films.

Table 1 shows the chemical compositions of the resultant films as determined by ICP-AES. Compositional comparison of the as-sprayed film and resultant film shows that the stoichiometric variation of Bi and Pb constituents in the film annealed in the closed system is smaller than that of Cu. But the compositional variation of Bi, Pb and Cu in the open system is largely different from that in the closed system. The difference is attributed to the compositional loss of Bi, Pb and Cu in the as-sprayed film in the closed system and can be compensated from the $Bi_{0.8}Pb_{0.2}SrCaCu_2O_y$ bulk source, whereas this is not possible in the open system. In general, the melts of Ca–Cu-containing compounds appearing in the superconductor ceramics flowed out and adhered to the carrier boat, which resulted in the higher compositional loss of Cu and Ca than Bi and Pb in the bulk ceramics. Excess amount of CuO and CaO [10] in the preparation of superconducting

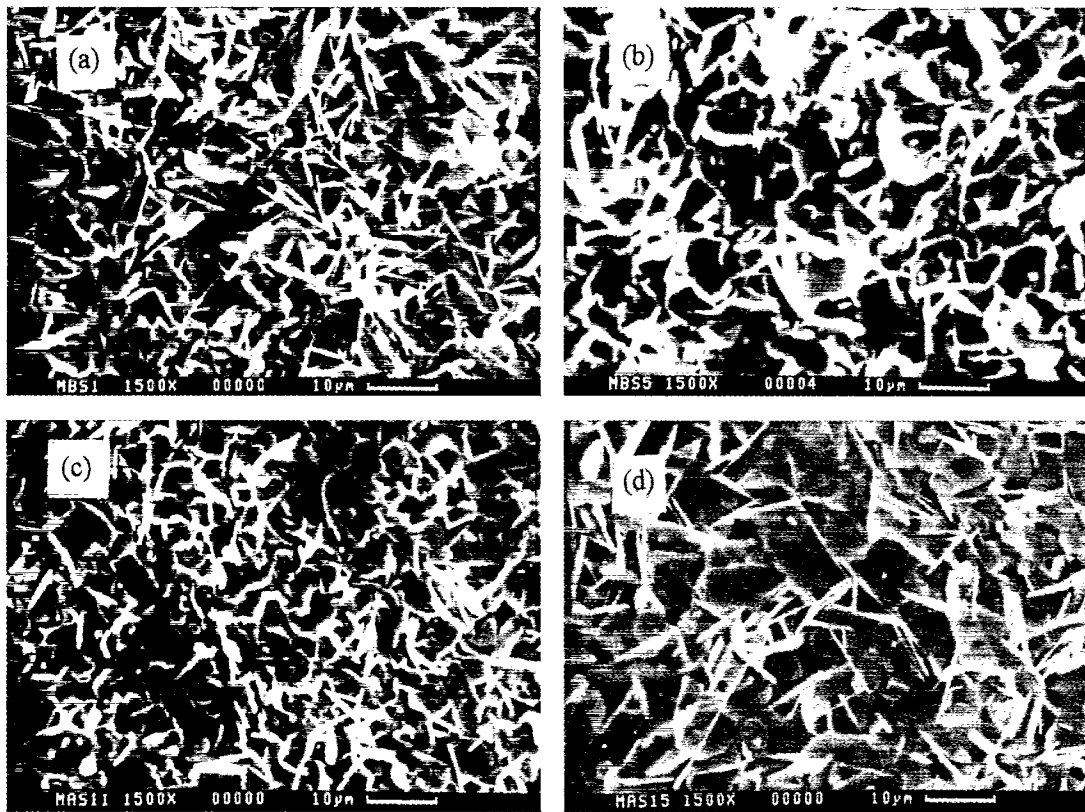


Fig. 6. SEM morphologies of the films A annealed at 840°C for 5 h (a), 50 h (b) and 850°C for 5 h (c), 50 h (d).

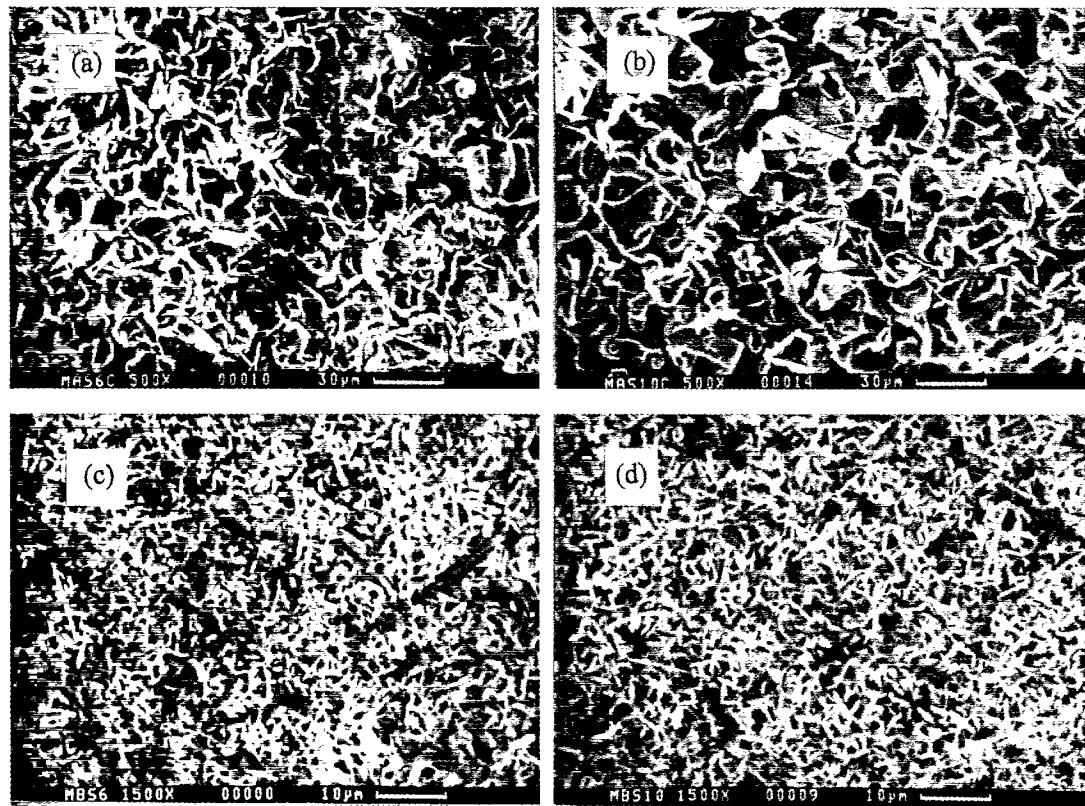


Fig. 7. Surface microstructures in the films A annealed in the closed system at 845°C for 5 h (a), 50 h (b) and in the open system at 845°C for 5 h (c), 50 h (d).

Table 1
Chemical compositions of the films A and B annealed at 845°C for 20 h in closed and open systems

Starting compositions	Processing conditions	Chemical composition of resultant films				
		Bi	Pb	Sr	Ca	Cu
$\text{Bi}_{1.8}\text{Pb}_{0.2}\text{Sr}_2\text{Ca}_2\text{Cu}_3\text{O}_y$	845°C (closed) for 20 h	1.91	0.19	1.97	2.12	3.16
	845°C (open) for 20 h	1.51	0.15	1.98	1.89	2.52
$\text{Bi}_2\text{Pb}_2\text{Sr}_2\text{Ca}_2\text{Cu}_3\text{O}_y$	845°C (closed) for 20 h	2.15	1.98	2.02	2.13	3.09

oxides has had a compensation effect on the formation of high- T_c 2223 phase for the vaporization and melting of Cu and Ca during the reaction. However, the compensation effect of the $\text{Bi}_{1.8}\text{Pb}_{0.2}\text{Sr}_2\text{Ca}_2\text{Cu}_3\text{O}_y$ bulk source on the as-sprayed films and prevention of evaporation of bismuth and lead in the closed system during the post-annealing reaction are evident. The dominating phases in the as-sprayed film B are CaCO_3 and SrCO_3 , in contrast to the CaCO_3 alone in the as-sprayed films A. The SrCO_3 phase appeared in the as-sprayed film A annealed at 500°C for 5 h and disappeared in the film annealed at about 700°C. The CaCO_3 and SrCO_3 phases appeared in the as-sprayed film B, indicating the decomposition of metal nitrates into carbonates in the preheated substrates during the spray deposition of metal nitrate at low temperature, as demonstrated by the exothermic peak at 100–200°C.

Fig. 9 shows XRD patterns of Ca_2PbO_4 in the films B annealed at 840°C for 5 h (a), 10 h (b), 20 h (c), 25 h (d) and 50 h (e). The intensity of Ca_2PbO_4 peaks in the films B annealed at 840°C gradually decreases when the processing time is increased and disappeared for 50 h. The film annealed at 840°C for 50 h shows nearly a single 2223 phase. The as-sprayed films annealed at 845°C for various periods show an increase of high- T_c 2223 phase and a decrease of Ca_2PbO_4 in the XRD relative intensities as the reaction time is increased. This phenomenon shows that the Ca_2PbO_4 phase plays a

critical role in the formation of high- T_c films along with the 2223 phase and several reports have proved the catalytic effect of Ca_2PbO_4 phases in the bulk [3,4,9].

Fig. 10(a) and (b) shows, respectively, the critical transition temperature ($T_{c,zero}$) and volume fraction of high- T_c 2223 phase for the films B annealed at 840 and 845°C for various periods. A high critical transition temperature of 104 K can be achieved for the films annealed at 840°C for 10 h and the volume fraction of high- T_c 2223 phase also increased with increasing treatment time. On the other hand, the critical transition temperature and volume fraction of high- T_c 2223 phase of films A annealed at 840°C for 10 h are 100 K and above 93%, respectively.

Fig. 11 shows SEM photographs of the films B annealed at 840 and 845°C. Both needle-like and plate-like microstructures appear in the films annealed at 840 and 845°C for 5 h (Fig. 11(a) and (c)), while the width and length of the

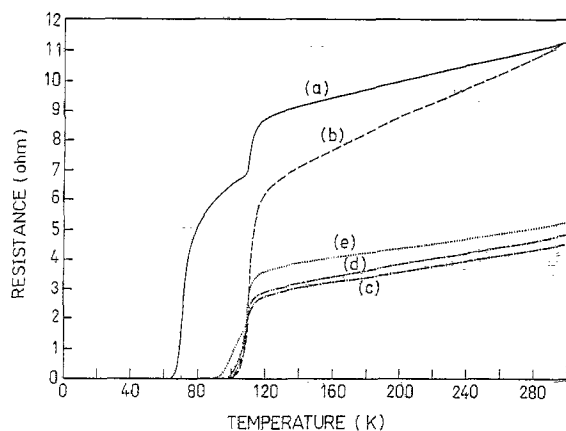


Fig. 8. Typical resistance-temperature relationship of the films A annealed at 840°C for 5 h (a), 10 h (b), 20 h (c), 25 h (d) and 50 h (e).

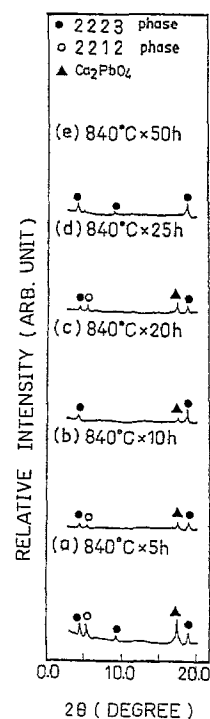


Fig. 9. XRD patterns of Ca_2PbO_4 phase in the films B annealed at 840°C for 5 h (a), 10 h (b), 20 h (c), 25 h (d) and 50 h (e).

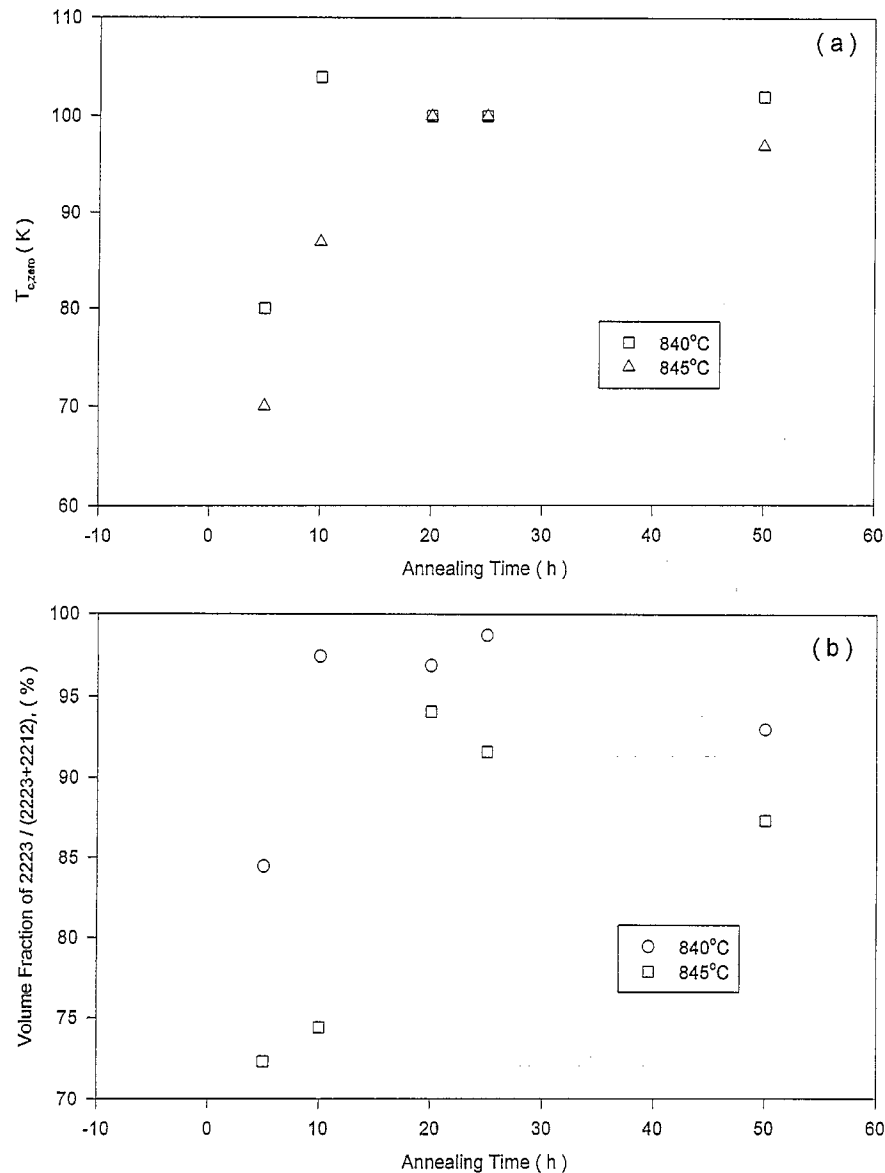


Fig. 10. (a) The critical transition temperature ($T_{c,zero}$) and (b) the volume fraction of high- T_c 2223 phase of the films B annealed at 840°C and 845°C for 5, 10, 20, 25 and 50 h.

plate-like microstructures increase with increasing processing time (Fig. 11(b) and (d)). On the other hand, the needle-like microstructures gradually decrease as the duration of annealing treatment is increased. These results explain that long-period annealing treatment at an appropriate range of temperatures is beneficial to the formation of high- T_c 2223 phases and is consistent with the reaction route in the film A along with Bi-based bulk.

Fig. 12 shows the voltage–current relationship for the film B (a) and film A (b) annealed at 840°C for 10 h. The transport critical current densities, J_c , of the resultant films at 77 K in zero magnetic field were calculated to be 1.8×10^4 and 2.2×10^3 A/cm² for films A and B, respectively. VanDover et al. [24] reported that a critical current density of 5×10^4 A/cm² has been measured for single-crystal Bi₂Sr₂CaCu₂O_y

in zero applied magnetic field and the critical current densities of the sample decreased with increasing magnetic field and vanished in a field of 5 kOe. A combination of rolling and uniaxial pressing with intermediate sintering on the Bi-2223 phase is effective not only for the Ag-sheathed tape but also for the screen-printed film, to obtain high J_{c0} values above 1×10^4 A/cm² (77 K, 0 T) [25] and the critical current density of Bi-based thin film and single crystal can be enhanced by irradiation and creating artificial pinning centres during the process of thin-film growth [26]. At present, the preparation of high- T_c Bi-based superconducting films by spray pyrolysis and post-annealing can also achieve comparable value with the above-mentioned Bi-based films without additional processing steps such as rolling, pressing and irradiation.

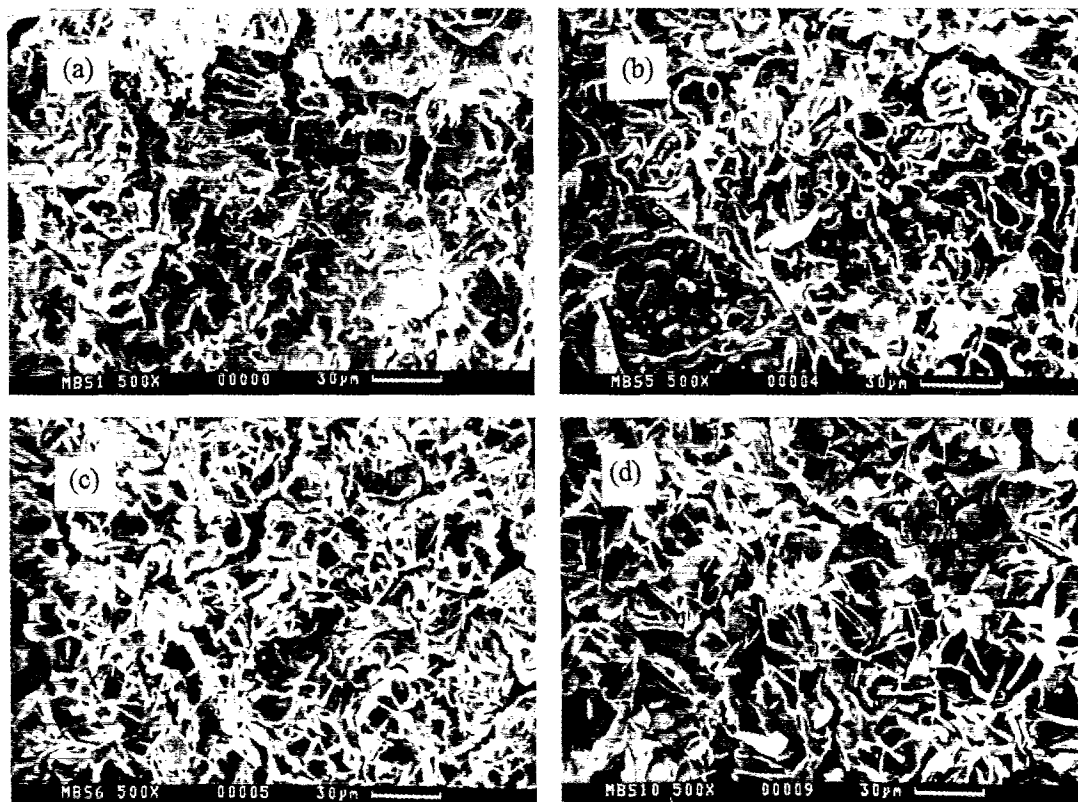


Fig. 11. SEM photographs of the films B annealed at 840°C for 5 h (a), 50 h (b) and at 845°C for 5 h (c), 50 h (d).

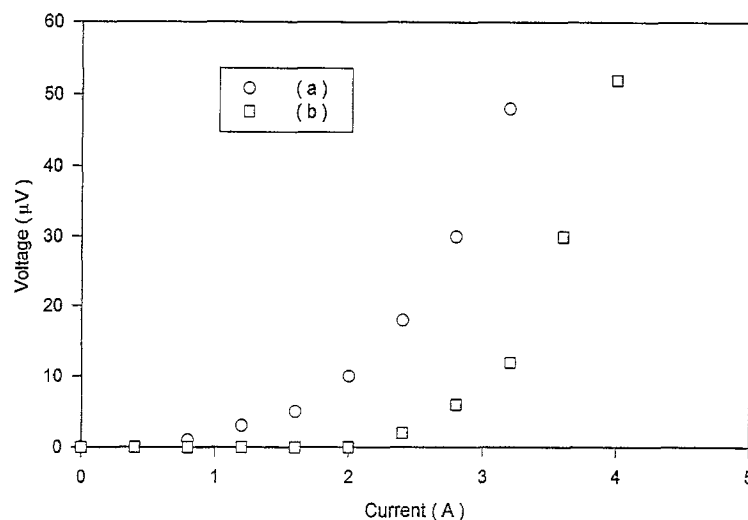


Fig. 12. Voltage–current relationship of the resultant films of $\text{Bi}_{1.8}\text{Pb}_{0.2}\text{Sr}_2\text{Ca}_2\text{Cu}_3\text{O}_y$ (a) and $\text{Bi}_{1.8}\text{Pb}_{0.2}\text{Sr}_2\text{Ca}_2\text{Cu}_3\text{O}_y$ (b) which were annealed at 840°C for 10 h.

4. Conclusions

Highly c -oriented and nearly high- T_c 2223 single-phase films were synthesized from as-sprayed films of $\text{Bi}_{1.8}\text{Pb}_{0.2}\text{Sr}_2\text{Ca}_2\text{Cu}_3\text{O}_y$ and $\text{Bi}_2\text{PbSr}_2\text{Ca}_2\text{Cu}_3\text{O}_y$ annealed at 845°C for 20 h. The amorphous as-sprayed films were crystallized and transformed into high- T_c (2223) phase, low- T_c (2212) phase and Ca_2PbO_4 during the annealing process, these phases being detected by means of XRD in the annealed films. The relative intensity of the Ca_2PbO_4 phase in the XRD

pattern gradually increased at annealing temperatures below 800°C, decreased at above 800°C and finally disappeared at 840–845°C, depending on the stoichiometric metal ratio. This indicates that the Ca_2PbO_4 phase plays a crucial role in the formation of high- T_c superconducting film as with the bulk. The as-sprayed films annealed in a closed system with a Bi-based bulk source are favourable for the preparation of the 2223 phase, whereas the 2212 phase is formed in the open system. The difference may be attributed to compensation and diffusion of constituents in the Bi-based bulk source into

as-sprayed films in the closed system. The 2223 phase has plate-like morphology and the 2212 phase needle-like morphology. A critical transition temperature of about 104 K and a critical current density around 1.8×10^4 A/cm² could be obtained in the 845°C-annealed film B.

Acknowledgements

This work is supported by the National Science Council of the Republic of China under project NSC 86-2112-M009-028.

References

- [1] E.J. Tomlinson, Z.H. Barber, G.W. Morris, R.E. Somekh, J.E. Evetts, *IEEE Trans. Mag.* 25 (1989) 2530.
- [2] M.R. Rao, E.J. Tarsa, H. Kroemer, A.C. Gossard, E.L. Hu, P.M. Petroff, W.L. Olson, M.M. Eddy, *Appl. Phys. Lett.* 56 (1990) 490.
- [3] T. Yoshitake, T. Satoh, Y. Kubo, H. Igarashi, *Jpn. J. Appl. Phys.* 27 (1988) L1262.
- [4] K. Natori, S. Yoshizawa, J. Yoshino, H. Kukimoto, *Jpn. J. Appl. Phys.* 29 (1990) L930.
- [5] T. Nabatame, Y. Saito, K. Aihara, T. Kamo, S. Matsuda, *Jpn. J. Appl. Phys.* 29 (1990) L1813.
- [6] S.P.S. Arya, H.E. Hintermann, *J. Less-Common Met.* 164–165 (1990) 478.
- [7] H.S. Koo, G.C. Tu, J.J. Chu, W.H. Lee, P.T. Wu, *Physica C* 9 (1990) 1326.
- [8] N. Tohge, M. Tatsumisago, T. Minami, K. Okuyama, M. Adachi, Y. Kousaka, *Jpn. J. Appl. Phys.* 27 (1988) L1086.
- [9] F.H. Chen, H.S. Koo, T.Y. Tseng, *Appl. Phys. Lett.* 58 (1991) 637.
- [10] N. Kijima, H. Endo, J. Tsuchiya, A. Sumiyama, M. Mizuno, Y. Oguri, *Jpn. J. Appl. Phys.* 27 (1988) L821.
- [11] U. Endo, S. Koyama, T. Kawai, *Jpn. J. Appl. Phys.* 27 (1988) L1476.
- [12] Y. Yamada, S. Murase, *Jpn. J. Appl. Phys.* 27 (1988) L996.
- [13] G.L. Messing, S. Zhang, G.V. Jayanthi, *J. Am. Ceram. Soc.* 76 (1993) 2707.
- [14] T. Konaka, I. Sankawa, T. Matsuura, T. Higashi, K. Ishihara, *Jpn. J. Appl. Phys.* 27 (1988) L1092.
- [15] H. Zhuang, H. Kozuka, T. Yoko, S. Sakka, *Jpn. J. Appl. Phys.* 29 (1990) L1107.
- [16] H.S. Koo, G. Tu, T.Y. Tseng, *J. Am. Ceram. Soc.* 77 (1994) 27.
- [17] M. Klee, J.W.C. de Vries, W. Brand, *Physica C* 156 (1988) 641.
- [18] P. Barboux, J.M. Tarascon, F. Shokoohi, B.J. Wilkens, C.L. Schwartz, *J. Appl. Phys.* 64 (1988) 6382.
- [19] T. Manabe, T. Tsunoda, W. Kondo, Y. Shindo, S. Mizuta, T. Kumagai, *Jpn. J. Appl. Phys.* 31 (1992) 1020.
- [20] H. Nasu, H. Nonogawa, A. Nozue, K. Kamiya, *Jpn. J. Appl. Phys.* 29 (1990) L450.
- [21] M. Kanai, T. Kawai, M. Kawai, S. Kawai, *Jpn. J. Appl. Phys.* 27 (1988) L1293.
- [22] T. Sata, K. Sakai, S. Tashiro, *J. Am. Ceram. Soc.* 75 (1992) 805.
- [23] T. Sata, K. Sakai, S. Tashiro, *J. Am. Ceram. Soc.* 74 (1991) 1445.
- [24] R.B. VanDover, L.F. Schneemeyer, E.M. Gyorgy, J.V. Waszczak, *Phys. Rev. B* 39 (1989) 4800.
- [25] A. Oota, H. Matsui, M. Funakura, J. Iwaya, J. Maeda, *Appl. Phys. Lett.* 63 (1993) 243.
- [26] V.V. Metlushko, G. Guntherodt, P. Wagner, H. Adrian, I.N. Goncharov, V.V. Moshchalkov, Y. Bruynseraede, *Appl. Phys. Lett.* 63 (1993) 2821.